JOURNAL OF CATALYSIS **163,** 122–129 (1996)
ARTICLE NO. 0311

# Characterization of VPO Catalysts by X-Ray Photoelectron Spectroscopy

G. W. Coulston,[1] E. A. Thompson, and N. Herron

*Central Research and Development E. I. duPont de Nemours, Inc. Experimental Station, Wilmington, Delaware 19880*

Received March 1, 1996; revised June 3, 1996; accepted June 7, 1996

**Methods are described for determining the P/V ratio and average vanadium oxidation state in vanadium phosphates using X-ray photoelectron spectroscopy. The determination of P/V ratios are based on a calibration derived from five organometallic complexes containing vanadium and phosphorus. The vanadium oxidation state is shown to be related to the splitting between O(1s) and V($2p_{3/2}$) transition centroids, $V_{ox} = 13.82 - 0.68\,[O(1s) - V(2p_{3/2})]$. A simple calculation is presented, which reveals that the layered structure of $(VO)_2P_2O_7$ can lead to an apparent 14% phosphorus enrichment when the surface is assumed to terminate with pyrophosphate groups. Exposure of $\beta$, $\gamma$, and $\delta$ $VOPO_4$ phases to increasing concentrations of butane in 10% $O_2/N_2$ results in transformation of the phases to vanadium pyrophosphate, as evidenced by the shifts in the P(2p) photoelectron transitions. During the transformation, the X-ray photoelectron spectroscopy P/V ratio in $\beta$-$VOPO_4$ increases by ca. 40%, whereas a much smaller increase is observed for the $\gamma$ and $\delta$ phases. As prepared and under oxidizing conditions, the surface of $\beta$ $VOPO_4$ has P/V < 1.** 

## INTRODUCTION

Vanadium pyrophosphate, $(VO)_2P_2O_7$, an exceptional catalyst for the oxidation of butane to maleic anhydride, has been studied from a variety of perspectives. Although many groups agree on the bulk structure of the catalytically active phase (1), there is little agreement about the nature of the active surface. X-ray photoelectron spectroscopy (XPS) has been used by many groups in an effort to determine the values of such potentially important parameters as the surface P/V ratio and the surface vanadium oxidation state. However, disagreement remains in the literature regarding the values of both of these surface properties for all of the studied vanadium phosphate phases. For example, most workers (2–6) seem to be in agreement that the surface P/V ratio of working catalysts is significantly enriched relative to the bulk value, although one literature report (7) suggests that surface P/V ratios are nearly 1 : 1. Regarding the oxidation state of surface vanadium, various interpretations have been assigned to the often broad and slightly asymmetric V($2p_{3/2}$) photoelectron transition (4, 6, 8, 9), but a clear picture has not emerged.

[1] To whom correspondence should be addressed.

The application of XPS to the characterization of metal oxide catalysts is complicated by the fact that the results of data analysis are not unique. There are several reasons for this, but the most prevalent are that it is not possible to determine the true background contribution to the spectrum, that final state effects in the photoemission process give rise to line shapes that are difficult to model rigorously, and that there are ubiquitous problems with sample charging and the often ignored Fermi level shifting due to, for example, changes in the oxygen vacancy defect concentration. Thus, some of the disagreement concerning the nature of the $(VO)_2P_2O_7$ surface may be due to variations in the subtleties of the data analysis and not necessarily due to differences in the samples themselves.

In this paper, we propose a simple procedure that is useful for determining the average vanadium oxidation state in vanadium oxides and phosphates, and we use it to characterize the $\beta$-, $\gamma$-, and $\delta$-vanadium phosphate phases after exposure to a variety of conditions. We also present a new procedure for calibrating the measurement of the P/V ratio of vanadium phosphate surfaces and show how the surface phosphorus concentration is affected by exposure of the catalysts to *n*-butane. We also present the first evidence for *vanadium* enrichment of the surface of some vanadium phosphates.

## EXPERIMENTAL

All of the XPS spectra were collected on a VG ESCAlab II spectrometer equipped with a standard polychromatic twin anode (Mg and Al) X-ray source and a 150-mm hemispherical analyzer. A stainless steel pretreatment cell was housed in the entry lock to the vacuum chamber. This setup allowed samples to be transferred between reactive and vacuum environments without room air exposure. The catalyst temperature was monitored during reaction using a K-type thermocouple, which was located inside of the cell and in contact with the catalyst. A UTI 100C mass-spectrometer was used to monitor the effluent from the pretreatment chamber. Nitrogen/helium tracer studies indicated that the cell could be considered a continuous stirred tank reactor (CSTR) for flow rates greater than 50 sccm. All gas flow rates were controlled using mass flow controllers (Tylan).



0021-9517/96 $18.00

**TABLE 1**

**Stoichiometries of VPO Organometallic Compounds**

| Cluster stoichiometry | Nominal P/V | $I_P/I_V$ |
|---|---|---|
| $(VO)_4(OCH_3)_6(HOCH_3)_2(O_2P(C_6H_5)_2)_2$ | 0.5 | 0.204 |
| $(VO_2CH_3)_4(P_2O_7)_2$ | 1 | 0.383 |
| $(VO)_4(C_6H_5PO_3)_4O_2F(P(C_2H_5)_4)$ | 1.25 | 0.510 |
| $(VO)_6(O_3POSi(CH_3)_3)_8Cl$ | 1.33 | 0.488 |
| $(VO)_3(O_2P(OC_2H_5)_2)_6(CH_3CN)$ | 2 | 0.746 |
| | | $A = 2.674$ |

The $\beta$, $\gamma$, and $\delta$ $VOPO_4$ phases were prepared and subsequently confirmed by X-ray diffraction as in Ref. 10. The $(VO)_2P_2O_7$ sample was prepared as described elsewhere (11). The $V_2O_5$ and vanadium foil were purchased from Aldrich. The vanadium and phosphorus containing organometallic complexes described in Table 1 were prepared as in Refs. 12 and 13. The $VO(H_2PO_4)_2$ was prepared as follows: 26.5 g (0.1 mole) vanadium (IV) bis (2,4-pentanedionate) was weighed into a clean beaker and 23.0 g (0.2 mole) 85% phosphoric acid was added directly to the green solid. The slurry was heated and stirred until it became a thick, homogeneous, dark-blue liquid. On continued warming the liquid began to evolve 2,4-pentanedione and suddenly solidified to a blue cake. At this point the sample was allowed to cool and the blue solid was recovered by slurrying into acetone and filtering. Following suction drying, the material was confirmed by XRD to be phase pure $VO(H_2PO_4)_2$ (JCPDS file card 40-38). Yield, 24.4 g, 94%. Approximately 10 g of $VO(H_2PO_4)_2$ was spread thinly in a clean quartz boat inside the quartz liner of a horizontal tube furnace and heated in a flow of 200 ml/min nitrogen. The temperature was ramped to 500°C over 1 h and held there for 24 h. The catalyst was then cooled and collected and the crystalline phase confirmed as $VO(PO_3)_2$ by XRD (JCPDS file card 33-1443). The powder diffractogram indicated a clean phase but the diffraction peaks are broad, indicating very small crystallite size. A nearly equivalent material could be prepared using a calcination atmosphere of air rather than nitrogen. The recovered powder showed an XRD pattern identical to that prepared in nitrogen, although XPS revealed that the surface of the air calcined sample contained approximately 20% $V^{5+}$. Attempts to reproduced the procedure given by Sananes *et al.* (5) using $V_2O_4$ dissolution in $H_3PO_4$ were unsuccessful, the products being extensively contaminated by V(V) phosphates according to XRD.

## RESULTS AND DISCUSSION

### *A. Determination of the Vanadium Oxidation State*

In principle, curve fitting V(2p) spectra to extract the distribution of vanadium oxidation states is possible; although, the problem in practice is quite complicated because vanadium II, III, and IV have partially filled valences. As a result, the interaction between the core-hole produced by photoemission and valence-holes in the partially oxidized cation will break the degeneracy of the sublevels in each 2p spin-orbit component. Gupta and Sen (14) have estimated the magnitudes of the multiplet splittings for vanadium final states with configurations of $2p^5d^1$, $2p^5d^2$, $2p^5d^3$, and $2p^5d^4$ states. Although their calculations ignored several important effects such as crystal field symmetry and instantaneous electron correlation, their results clearly showed that one should expect, at the very least, the peaks in a $V^{1+, 2+, 3+, \text{or } 4+}$ spectrum to be asymmetrically broadened toward higher binding energy, but that it would more likely be the case that the 2p transition manifest itself as a quartet rather than a doublet. In any case, the high binding energy shoulder in $V(2p_{3/2})$ XPS spectra of reduced samples could then easily be misinterpreted as a contribution from the next higher state of oxidation. Thus one simply cannot use the same lineshape for $V^{2+}$, $V^{3+}$, and $V^{4+}$ as used for $V^{5+}$ and still hope to get meaningful results. Furthermore, considering the surface sensitivity of XPS and the tendency of vanadium to oxidize upon exposure to ambient conditions, it would be difficult to develop a suitable set of standards for each valence. Fortunately, while multiplet splitting is expected to significantly affect the lineshapes of the $V(2p_{1/2})$ and $V(2p_{3/2})$ spin orbit components, the centroids of these components are not expected to be affected. Thus our approach has been to employ a spectral moment analysis to determine the average vanadium oxidation state in a spectrum. In doing so, we accept that we will not be able to determine the distribution of vanadium oxidation states in a sample without additional information, but we also recognize that knowledge of the average value is often sufficient.

We developed the calibration shown in Fig. 1 for extracting the average vanadium oxidation state in a $VO_x$ sample from the splitting between the O(1s) and $V(2p_{3/2})$ centroids. The centroids were determined as described in the Appendix. To arrive at Fig. 1, we started with dry $V_2O_5$, obtained by heating a $V_2O_5$ sample in dry air at 400°C in the pretreatment cell for several hours, followed by cooling to 25°C in dry air before removing the sample from the pretreatment cell. A $V_2O_5$/V sample was also prepared by identically treating a vanadium foil. It has been reported (15) that stable native oxides on vanadium substrates are difficult to grow due to the facile diffusion of oxygen into the bulk at some conditions. However, the lack of appreciable bandgap emission in the He II UPS spectrum in Fig. 2a supports our claim that the oxide overlayer produced in our experiment was V(V). In addition, the three peaked structure of the UPS spectrum is comparable to that measured by Zhang and Henrich (16) on a $V_2O_5(001)$ surface. The two samples were then sputtered with 4.5-kV $Ar^+$ ions in order to cause a reduction of the vanadium (17). The O/V

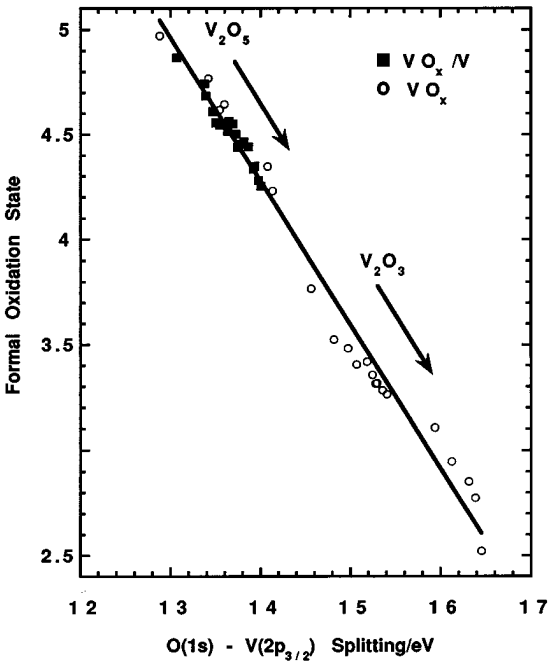


**FIG. 1.** Vanadium oxidation state calibration curve. The first order least-squares fit can be described $V_{ox} = 13.82 - 0.68\,[O(1s) - V(2p_{3/2})]$. The starting material for the powered samples is indicated in the figure.

atomic ratio, measured at various times during the sputtering process, was related to the average vanadium oxidation state by comparison to the O/V ratio measured for the unsputtered $V_2O_5$ powder sample. Although preferential sputtering of oxygen will result in a depth profile of vanadium in various oxidation states, this should have no affect on our determination of the average stoichiometry because the photoelectron attenuation lengths for V(2p) and O(1s) photoelectrons are identical. In order to access vanadium oxidation states lower than $V^{3+}$, it was necessary to start with a $V_2O_3$ sample. However, in this latter case, the relative cross sections of the O(2p) and V($2p_{3/2}$) transitions were still based on $V_2O_5$. The linear dependence between formal oxidation state and centroid splitting observed in Fig. 1 is consistent with first order treatments of the photoelectron process based on Hartree–Fock theory (18).

To compare our results to those of others, we should like to know the shift in the V($2p_{3/2}$) binding energy upon reduction from $V^{5+}$ to $V^{4+}$. To do this requires that we determine absolute binding energies for the V($2p_{3/2}$) peak, although such knowledge is not required to use our calibration. Energy referencing to C(1s) is not reliable on our samples because their *in situ* preparation results in very low carbon levels. Also, one cannot be certain of the chemical state of the carbonaceous overlayer, especially when trying to compare samples with vanadium in different oxidation states. However, we can estimate the change in V($2p_{3/2}$) binding energy between $V^{5+}$ and $V^{4+}$ by first accounting for the shift in the O(1s) binding energy upon reduction. Figure 2b shows the He II UPS spectrum of the Vox/V sample after sputtering. The shift in the top of the valence band, which is due primarily to nonbonding orbitals on the oxygen, is approximately 0.45 eV. In a rigid band theory, the same shift would apply to the O(1s) orbitals. By XPS, the increase in the centroid splitting upon sputtering was 1.17 eV, suggesting a V($2p_{3/2}$) shift of 0.72 eV ($= 1.17$ eV $- 0.45$ eV) upon reduction. The oxidation state of the reduced sample was determined to be 4.2 by XPS, indicating an average spitting between $V^{5+}$ and $V^{4+}$ of 0.9 eV ($= 0.72/0.8$). This value is in good agreement with the values of 1 and 0.7 eV reported in Refs. 19 and 20, respectively.

Since the calibration was developed for vanadium oxides of the form $VO_x$, one can question whether it should be useful for vanadium phosphates. Again, the only standards in which we can have absolute confidence are those of V(V). Applying our calibration to air calcined $\beta$-$VOPO_4$, $\gamma$-$VOPO_4$, and $\delta$-$VOPO_4$ samples, respectively, gives $V_{ox} =$ 5.0, 5.02, and 5.04. Values so close to 5.0 suggest that, the calibration is valid for fully oxidized vanadium phosphates. To further validate our method, we have used it to determine the average oxidation state of vanadium in $(VO)_2P_2O_7$ after exposure to a 10% butane/helium mixture for 90 min at 500°C. This treatment removed all of the oxygen energetically accessible to butane at 500°C. Analysis of this material by XPS yielded an average surface vanadium oxidation state of 3.65. Chemical titration (21) of the same sample indicated an average vanadium oxidation state of 3.7, in very good agreement with the value determined by XPS.

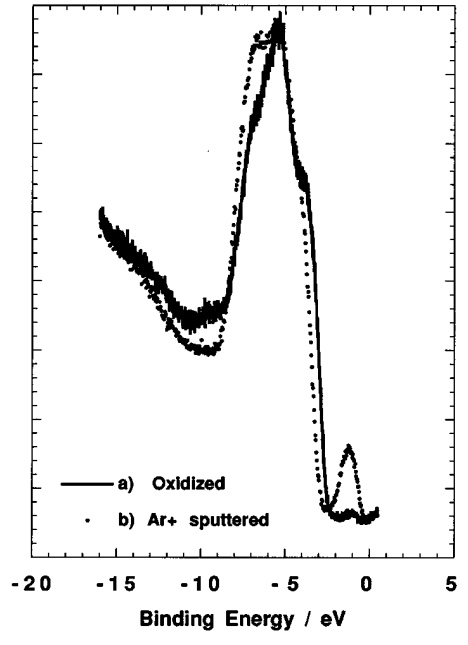


**FIG. 2.** He II UPS of $V_{ox}$/V after oxidation (a) and following 4.5-keV $Ar^+$ sputtering (b). The small emission in the band gap of the oxidized sample is a satellite of the $1b_2$ orbital of $H_2O$ appearing at −9.6eV.

Thus we conclude that our method is useful for vanadium phosphates as well as for vanadium oxides.

We wish to note, however, that when an excessive amount of water is incorporated into the sample, such as in $VOPO_4 \cdot H_2O$, a shoulder begins to appear on the high binding energy side of the O(1s) transition, and the calibration begins to err toward lower vanadium oxidation states since the O(1s)–V($2p_{3/2}$) peak splitting becomes enhanced. However, we have not found this to be a problem in most of our work since the samples we analyze typically are not hydrates and a partial monolayer of hydroxyl groups on oxide surfaces is virtually undetectable by XPS. However, consistent with published reports (5), a significant hydroxyl concentration (ca. 10% of O(1s) peak) was observed in the $VO(PO_3)_2$, regardless of the calcination procedure. In such cases with comparable levels of hydroxyl content, as determined by O(1s) XPS, we find that our method is useful for measuring differences in vanadium oxidation state between samples.

### *B. Determination of the P/V Ratio*

The P/V atomic ratio ($N_P/N_V$) of a vanadium phosphate can be measured in an XPS experiment as a function of the intensity ratio ($I_P/I_V$), spectrometer transmission function ($T$), electron attenuation lengths in the sample ($\lambda$), and photoemission cross sections ($\sigma$). Both $T$ and $\lambda$ depend primarily on the kinetic energy of the emitted electron, while $\sigma$ also depends on the principal and orbital angular momentum quantum numbers of the photoelectron prior to emission, as well as on the angle of emission measured relative to the path of the incident X-rays. Provided the experiment geometry, X-ray photon energy, and all analyzer settings are kept constant, one can simply consider $N_P/N_V = A(I_P/I_V)$. Determination of the scaling factor $A$ is straightforward, in principle, by using as a standard a sample with a known surface P/V ratio. However, if phosphorus segregation is considered a possibility in $(VO)_2P_2O_7$, then it should also be considered a possibility in other VPO compounds with extended structures, regardless of the crystallinity of those structures. Thus finding a suitable set of standards presents a problem.

To escape this conundrum, we have made use of a series of organometallic VPO compounds of varying phosphorus and vanadium stoichiometry. Each sample was characterized complete with its full complement of ligands. Since these samples crystallize as discrete molecular units, unlike the extended structures of $VOPO_4$ and $(VO)_2P_2O_7$, phosphorus segregation should not occur. Table 1 gives the stoichiometries of the clusters and measured P/V intensity ratios. The intensity of the V($2p_{3/2}$) peak was determined as described in the Appendix, while a simple straight line background subtraction and integration has been used to define the P(2p) peak. The data contained in Table 1 are plotted in Fig. 3, where one can see that the results fall nicely on a single calibration line. We have also included in Fig. 3 the calibration that we calculate using Scofield cross sections, Tanuma's correlation for the mean free paths of V(2p) and P(2p) photoelectrons (22), and the transmission function determined for our spectrometer. Based on the differences shown in Fig. 3, it is not surprising that so much controversy exists in the literature over the value of the surface P/V ratio. We have most confidence in our calibration based on molecular clusters since phosphorus segregation is not expected to occur in such compounds. However, structural heterogeneity can also induce an apparent enrichment in one of the sample components: alternating vanadium-rich and phosphorus-rich layers in the crystals could give rise to such an effect. We do not believe that this effect is manifest in this work because five clusters, with very different structures, yield the same calibration.

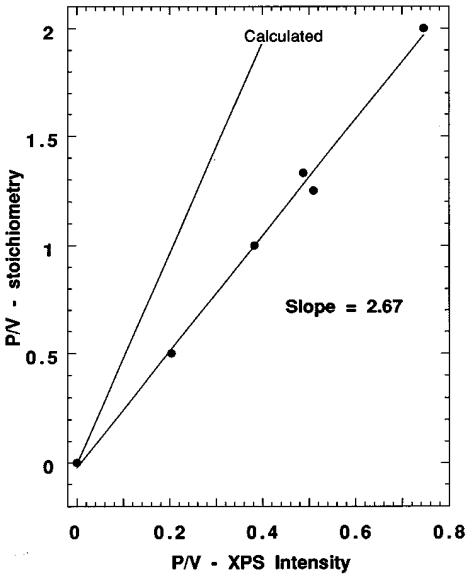


**FIG. 3.** XPS calibration for determination of P/V ratio. The data points were determined using the clusters described in Table 1. The calculated line was determined as described in the text.

Table 2 provides the P/V ratios determined for several commonly referred to phases of vanadium phosphate. Notice that the surface P/V ratio is, in all cases, very close

**TABLE 2**

**P/V Ratios of Several Common Phases of Vanadium Phosphate**

| Phase | Nominal P/V | XPS measured P/V |
|---|---|---|
| $\beta$-$VOPO_4$ | 1 | 0.85 |
| $\gamma$-$VOPO_4$ | 1 | 1.02 |
| $\delta$-$VOPO_4$ | 1 | 0.97 |
| $(VO)_2P_2O_7$ | 1 | 1.08 |
| $VO(PO_3)_2$ | 2 | 2.00 |
| $VO(H_2PO_4)_2$ | 2 | 2.22 |

to the value expected based on the bulk stoichiometry, and we do not find the factor of two enrichment commonly reported for $(VO)_2P_2O_7$ (2–4, 6) and $VO(PO_3)_2$ (5). Our determination of the surface stoichiometry of $(VO)_2P_2O_7$ is much more consistent with that reported by Misono *et al.* (7) using a calibration based on vanadium phosphate glasses. Also notice that the surface of the $\beta$-$VOPO_4$ phase is actually enriched in *vanadium*, not phosphorus, while the surfaces of $\gamma$ and $\delta$-$VOPO_4$ both have P/V ratios near unity. Interestingly, Zhang-lin *et al.* (23) have shown that $\gamma$- and $\delta$-$VOPO_4$ have similar selectivities for maleic anhydride production (ca. 60%), while that for $\beta$-$VOPO_4$ is much lower (ca. 24%). Perhaps the poor performance of $\beta$-$VOPO_4$ results from the increased vanadium surface concentration relative to the other $VOPO_4$ phases. However, that the performance of a $(VO)_2P_2O_7$ catalyst initially improves dramatically with time on stream while the surface P/V ratio remains nearly constant (6), can be taken as evidence that the surface P/V ratio alone does not serve as a predictor of catalyst performance. Clearly, one would like to known the surface structures of these various phases and not just the surface stoichiometries, but this cannot be done with standard XPS techniques on polycrystalline samples. We should also point out that at most 25% of the XPS signal is expected to originate from the outer 5 Å of the sample. This estimate is based on an approximation for the V(2p) mean free path, and it represents an upper bound since elastic scattering is expected to disproportionately increase the contribution of deeper layers. Thus small changes in surface stoichiometry/structure, which could have a profound affect on catalysis, can go unnoticed in an XPS experiment.

As mentioned above, the anisotropic structures of the vanadium phosphates can make the surface P/V ratio, as determined by XPS, sensitive to crystallite morphology. To estimate the magnitude of this effect, we have calculated the P/V ratio that one should expect to measure for $(VO)_2P_2O_7$ when viewed through the (100), (021), and (001) surfaces. The calculation involves adding the contributions from each element along the chosen direction, each contribution attenuated based on the appropriate mean free path. The crystal structure used is that reported by Ebner (24) and elastic mean free paths for $V(2p_{3/2})$ and P(2p) photoelectrons of 15 and 20 Å, respectively, were chosen based on Penn's model (22). The results are provided in Table 3. Note that two values are given for the P/V ratio along the (100) direction. This arises because of the choice of phosphorus termination; phosphate termination yields 1.098, while pyrophosphate termination yields 1.136. Thus one must be careful when interpreting correlations between performance and small changes in surface P/V ratio of a given phase. The result may be due more to changes in crystallite morphology than to changes in the P/V ratio of a given surface. On the other hand, trying to relate changes in P/V ratio to crystallite morphology is expected to be a heroic exercise since the XPS results will depend on the orientation of the crystals when they are mounted for study. Finally, Ebner and Thompson (24) earlier speculated that the phosphorus enrichment widely reported for $(VO)_2P_2O_7$ catalysts could be accounted for by pyrophosphate termination of the crystallites. However, they were trying to rationalize P/V ratios observed to be in excess of 1.5. As we show in Table 3, except for very thin crystallites (<20 Å), pyrophosphate termination on the (100) crystal face cannot account for a surface enrichment greater than 14%.

**TABLE 3**

**Calculated Dependence on Morphology of the P/V Ratio for $(VO)_2P_2O_7$**

| Orientation | 100 | 021 | 001 |
|---|---|---|---|
| P/V | 1.098–1.136 | 1.015 | 0.986 |

### *C. Dependence of P/V Ratio on Oxidation State*

Since P/V ratios are typically reported for vanadium phosphate catalysts with the goal of relating catalyst performance to the surface phosphorus content, it is important to consider the effect of reaction on the P/V ratio. Most reaction studies reported in the literature are under fairly mild conditions, e.g., 1.5% butane/air and temperatures below 450°C. In order to better determine the relationship between the surface P/V ratio and the vanadium oxidation state, we have performed a series of experiments with reactor feeds ranging from 0% $C_4H_{10}$/10% $O_2$/90% $N_2$ to a high of 30% $C_4H_{10}$/7% $O_2$/63% $N_2$ at 400°C. Samples were kept under reaction conditions for 1 h. In each case, the sample was removed from the reactor while still hot and allowed to cool in vacuum. It was necessary to allow the samples to cool below 50°C before a steady surface charge could be obtained during the XPS measurements. The P/V ratios and vanadium oxidation states determined for $\beta$, $\gamma$, and $\delta$ forms of $VOPO_4$ are given in Table 4.

**TABLE 4**

**Dependence of P/V Ratio on Extent of Reduction at 400°C**

| | $\beta$-$VOPO_4$ | | $\delta$-$VOPO_4$ | | $\gamma$-$VOPO_4$ | |
|---|---|---|---|---|---|---|
| %$C_4H_{10}$ | P/V | $V_{ox}$ | P/V | $V_{ox}$ | P/V | $V_{ox}$ |
| 0 | 0.91 | 4.72 | 0.97 | 5.04 | 1.01 | 5.02 |
| 1.5 | 0.88 | 4.63 | 1.01 | 4.91 | 1.02 | 4.97 |
| 5 | 0.98 | 4.42 | 1.10 | 4.76 | 1.01 | 4.89 |
| 10 | 1.15 | 4.29 | 1.07 | 4.46 | 1.03 | 4.66 |
| 20 | 1.42 | 3.98 | 1.06 | 3.88 | 1.08 | 3.87 |
| 30 | 1.39 | 3.73 | 1.04 | 3.86 | 1.09 | 3.77 |

*Note.* The leftmost column indicates the concentration of butane in a feed stream balanced by 10% $O_2/N_2$.

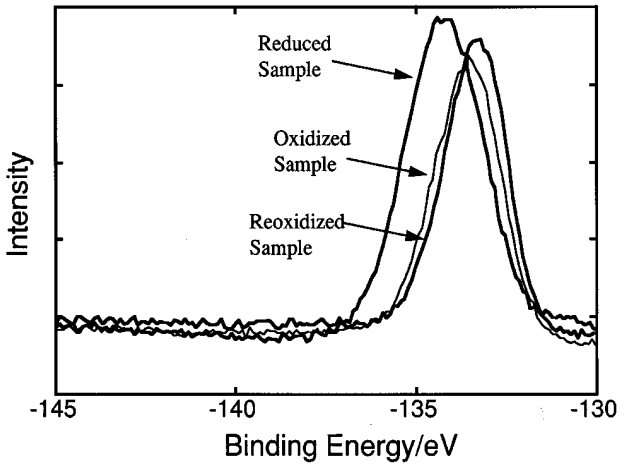


**FIG. 4.** Phosphorus (2p) photoelectron spectra of reduced (30% $n$-$C_4H_{10}$/10% $O_2/N_2$) and oxidized (10% $O_2/N_2$) $\beta$-$VOPO_4$. Oxidizing and reducing treatments lasted 1 h at 400°C. The spectra were collected following exposure to oxidizing, then reducing, and then oxidizing conditions.

The results clearly show that the surface P/V ratio measured on $\beta$-$VOPO_4$ is very dependent on the degree of reduction of the material. The surfaces of $\delta$ and $\gamma$ forms are far less sensitive. When viewing Table 4, one should keep in mind that XPS intensity ratios are seldom more precise than ±5% due to the somewhat subjective nature of the baseline determination. In Fig. 4, we show the P(2p) XPS spectra collected sequentially for oxidized (0% $C_4H_{10}$), reduced (30% $C_4H_{10}$), and reoxidized (0% $C_4H_{10}$) $\beta$-$VOPO_4$. The increase in the P/V ratio is clearly evidenced in Fig. 4, as is the shift of the P(2p) peak toward higher binding energy upon reduction. The shift is consistent with formation of P–O–P linkages, such as those found in vanadium pyrophosphate, and it is reversible. Similar shifts were observed for the $\gamma$ and $\delta$ phases, although they occurred without significant P segregation. We have used C(1s) charge referencing to determine the shifts in the P(2p) transitions, and we are aware of the potential inaccuracies inherent in such a technique. However, the C(1s) lineshapes were similar in all samples, suggesting that the nature of the carbon did not differ between samples. Thus while we have confidence in the magnitudes of the shifts observed in P(2p) spectra, we cannot be certain with our placement of the C(1s) transition at 284.6 eV. X-ray diffraction of similarly reduced samples confirms the transformation of each phase to $(VO)_2P_2O_7$ upon reduction. Finally, it is interesting to note that Zhang-Lin *et al.* (25) report conversion of $\beta$-$VOPO_4$ to $(VO)_2P_2O_7$ when the former is reduced by butadiene, whereas it was reported that $\gamma$, and $\delta$-$VOPO_4$ developed traces of the $\alpha_{II}$-$VOPO_4$ phase. We wish to point out here that for the P/V ratios we report in Table 4 for $\beta$-$VOPO_4$ to be consistent with growth of $(VO)_2P_2O_7$, the basal plane of $(VO)_2P_2O_7$ should be the predominant surface and the crystallites should be of order 20 Å thick so that both surfaces of the crystallite contribute to the XPS signal. Thicker crystallites would be expected to have P/V ratios approaching the values given in Table 3.

While addressing the effect of sample reduction on phosphorus enrichment, we should mention some of the systematic errors that can arise in such experiments that might also account for the result. Carbon contamination will tend to increase the measured P/V ratio because the slower moving $V(2p_{3/2})$ photoelectrons will be scattered more efficiently than those resulting from the P(2p) excitation. However, such contamination is not the cause of the increase here because, as shown in Fig. 5, the C(1s) signal was nearly constant for experiments with increasing butane exposures. The results in Fig. 5 also suggest that systematic errors in the integration of the $V(2p_{3/2})$ peak cannot be the result of the enrichment; the enrichment is largely an increase in the P(2p) signal and not a decrease in $V(2p_{3/2})$. Such error might result from not subtracting the true background from the spectrum before integration because the true background simply is not known and because the peaks are not baseline resolved. Furthermore, all of the $VOPO_4$ samples were reduced to comparable levels, yet only the surface of the $\beta$ phase became enriched. A third reason the apparent enrichment might have been an artifact can also be dismissed, i.e., that changes in the photoelectron mean free paths upon reduction of the catalyst change the relationship between intensity and concentration. For example, using the relationship for the inelastic mean free path given by Tanuma *et al.* (22) and the relationship given by Seah (26) between the inelastic mean free path and the electron attenuation length (which actually determines the sampling depth), assuming the vacancies created upon reduction are quenched by growth of shear planes thus increasing the density of the crystallites, and allowing the bandgap to decrease linearly with increasing reduction to $E_g = 0$ eV for $V^{2+}$ (based on VO) and $E_g = 3$ for $V^{5+}$ (based on He I UPS spectra),

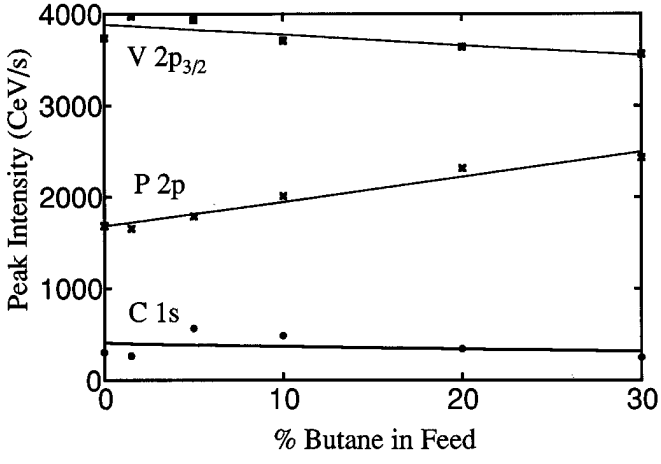


**FIG. 5.** Phosphorus, vanadium, and carbon levels on $\beta$-$VOPO_4$ as a function of butane concentration in a feed balanced by 10% $O_2/N_2$.

we calculate that the measured P/V ratio would actually *decrease* upon reduction, contrary to observation. Furthermore, the decrease is expected to be only <0.1%, far below the accuracy of even the most careful XPS measurements.

Thus it is clear that one should be careful when reporting surface P/V ratios to specify precisely the conditions to which the sample was exposed, and not merely the conditions of the preparation. These results also have implications for determining the kinetics of butane oxidation in unsteady processes. For example, in DuPont's riser reactor process for butane oxidation (27), vanadium phosphate catalysts are cycled between reducing and oxidizing conditions. The results reported here suggest that under such conditions, one might expect cyclical changes in the surface structure, and hence in the intrinsic rate constants associated with certain of the elementary reaction steps. As discussed elsewhere (28), this can serve to complicate the development of kinetic models and can force one to forego the concept of rate constants that are independent of species concentrations.

## CONCLUSIONS

Through application of XPS to the characterization of vanadium phosphates, we have shown that the surface P/V ratios of vanadium phosphate and pyrophosphate catalysts are much closer to the bulk value than previously found by most practitioners. We suspect that claims in the literature of gross phosphorus enrichment on these materials have been based on incorrect XPS calibrations. Furthermore, our results show that the surface of $\beta$-$VOPO_4$ is actually enriched in vanadium.

We have presented a method for extracting oxidation states from XPS spectra of vanadium oxides and vanadium phosphates that does not require curve fitting. Although it has the disadvantage of only providing the average oxidation state, it is not affected by surface charging and final state effects in the photoemission process, and it is the first XPS analysis of vanadium phosphates to account for such effects. Furthermore, when samples with small differences in the vanadium oxidation state are being compared, such as the differences shown in Table 4, the results of our method are likely to be more reliable than curve fitting.

We have shown that the surface P/V ratio in $\beta$-$VOPO_4$ is sensitive to the degree of reduction of the surface, much more so than found for either $\gamma$- or $\delta$-$VOPO_4$. The enrichment observed upon reduction appears to be reversible, although the claim of true reversibility will need to await experiments involving many more redox cycles. This effect has implications for kinetic modeling in unsteady systems: when the surface structure/stoichiometry responds with a time constant comparable to the characteristic time scale of the process transients, one must question the use of concentration independent rate constants in kinetic models.

## APPENDIX

Our procedure for analyzing the O(1s) and V(2p) region of the XPS spectrum involves first removing the Mg $K\alpha$ satellites by deconvolution, followed by removal of a Shirley background. The latter is defined by endpoints chosen above and below the O(1s) and V($2p_{3/2}$) peaks, respectively. Various satellite removal schemes are common; the parameters we use are those reported in Ref. 29, with added parameters for the $K\alpha'$ satellite based on the work of Krause and Ferreira (30).

Klauber (31) has recently revisited the Mg $K\alpha$ satellite structure and notes the importance of accounting for the varying linewidths of the satellite peaks, as well as the respective peak amplitudes. However, since it is a common practice to remove the satellites by deconvolution, accounting for the linewidths requires the introduction of an apodization function which effectively smoothes the spectrum. To avoid this smoothing, and to keep the analysis as simple as possible, we have assumed that all spectral lines of the X-ray source have the same lineshape. The result of the above operations on a spectrum of $V_2O_5$ is shown in Fig. A1.

The integrated intensity of a transition (zeroth order moment) is extracted from a filtered and Shirley background removed spectrum by drawing a secondary baseline. This is necessary because removal of the Shirley background does not result in baseline resolved peaks. The secondary

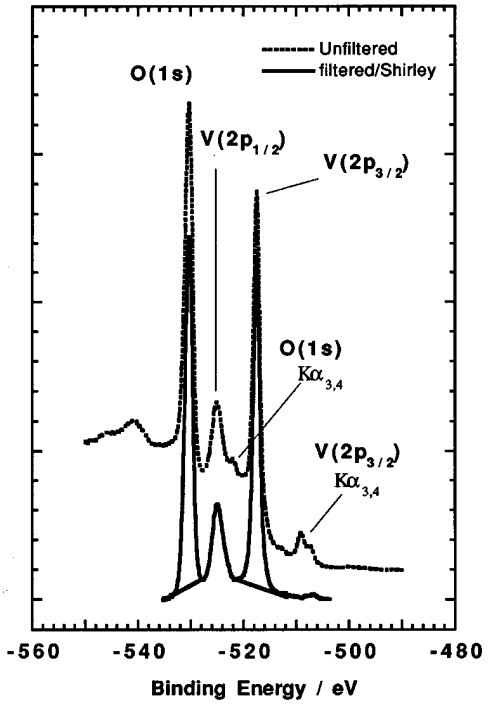


**FIG. A1.** Vanadium pentoxide XPS spectrum. The broken line represents the data as collected, while the solid line results after removing the X-ray satellites and Shirley background as described in the Appendix. The secondary baseline is also shown on the modified spectrum.

baseline for the O(1s) peak is drawn from the intensity minimum between the O(1s) and V($2p_{1/2}$) peaks toward higher binding energy and the baseline for the V($2p_{3/2}$) peak extends from the intensity minimum between the V($2p_{1/2}$) and V($2p_{3/2}$) peaks toward lower binding energy. It is interesting to note that applying this procedure to $V_2O_5$ yields an O/V ratio of 2.59 using calculated photoemission cross sections (32), which is close to the expected value of 2.5. Higher order moments can also be approximated for each transition using the same secondary background.

## ACKNOWLEDGMENTS

We gratefully acknowledge our colleagues D. Thorn and K. Kourtakis for providing some of the samples reported on in this paper.

## REFERENCES

1. Centi, G., *Catal. Today* **16**, 5 (1993).
2. Sola, G. A., Pierini, B. T., and Petunchi, J. O., *Catal. Today* **15**, 537 (1992).
3. Trifiro, F., *Catal. Today* **16**(1), 91 (1993).
4. Cornaglia, L. M., Caspani, C., and Lombardo, E. A., *Appl. Catal.* **74**, 15 (1991).
5. Sananes, M. T., Hutchings, G. J., and Volta, J. C., *J. Catal.* **154**, 253 (1995).
6. Abon, M., Bere, K. E., Tuel, A., and Delichere, P., *J. Catal.* **156**, 28 (1995).
7. Okuhara, T., and Misono, M., *Catal. Today* **16**(1), 61 (1993).
8. Shimoda, T., Okuhara, T., and Misono, M., *Bull. Chem. Soc. Jpn.* **58**, 2163 (1985).
9. Moser, T. P., and Schrader, G. L., *J. Catal.* **104**, 99 (1987).
10. Abdelouahab, F. B., Olier, R., Guilhaume, N., Lefebvre, F., and Volta, J. C., *J. Catal.* **134**, 151 (1992).
11. Horowitz, H., Blackstone, C., Sleight, A., and Teufer, G., *Appl. Catal.* **38**, 193 (1988).
12. Herron, N., Thorn, D., and Harlow, R., *Proc. Mater. Res. Soc.* **351**, 31 (1994).
13. Thorn, D. L., Harlow, R. L., and Herron, N., *Inorg. Chem.* **34**, 2629 (1995).
14. Gupta, R. P., and Sen, S. K., *Phys. Rev. B* **12**, 15 (1975).
15. Welter, J.-M., and Wachendorf, H.-N., *Appl. Surf. Sci.* **14**, 173 (1982–1983).
16. Zhang, Z., and Henrich, V. E., *Surf. Sci.* **321**, 133 (1994).
17. Kim, K. S., Baitinger, W. E., Amy, J. W., and Winograd, N., *J. Electron Spectrosc. Relat. Phenom* **5**, 351 (1974).
18. Cardona, M., and Ley, L., *in* "Topics in Applied Physics," (M. Cardona and L. Ley, Eds.), Vol. 26. Springer-Verlag, Berlin, 1978.
19. Rao, C. N. R., Sarma, D. D., Vasudevan, S., and Hegde, M. S., *Proc. R. Soc. London A* **367**, 239 (1979).
20. Sawatzky, G. A., and Post, D., *Phys. Rev. B.* **20**, 1546 (1979).
21. Centi, G., Fornasari, G., and Trifiro, F., *J. Catal.* **89**, 44 (1984).
22. Tanuma, S., Powell, C., and Penn, D., *Surf. Interface Anal.* **11**, 577 (1988).
23. Zhang-Lin, Y., Forissier, M., Sneeden, R. P., Vedrine, J. C., and Volta, J. C., *J. Catal.* **145**, 256 (1994).
24. Ebner, J. R., and Thompson, M. R., *Stud. Surf. Sci. Catal.* **67**, 31 (1991).
25. Zhang-Lin, Y., Forissier, M., Vedrine, J. C., and Volta, J. C., *J. Catal.* **145**, 267 (1994).
26. Seah, M. P., *in* "Practical Surface Analysis" (D. Briggs and M. P. Seah, Eds.). Wiley, New York, 1990.
27. Stadig, W., *Chem. Proc.* **August 27–31** (1992).
28. Coulston, G. W., Mills, P. L., and Sullivan, J., in preparation.
29. Wagner, C. D., Riggs, W. M., Davis, L. E., and Moulder, J. F., "Handbook of X-ray Photoelectron Spectroscopy." Perkin-Elmer Corporation, Eden Prairie, MN, 1979.
30. Krause, M. O., and Ferreira, J. G., *J. Phys. B.* **8**, 2007 (1975).
31. Klauber, C., *Appl. Surf. Sci.* **70/71**, 35 (1993).
32. Scofield, J. H., *J. Elect. Spec. Rel. Phen.* **8**, 129 (1976).